

## On the efficiency of ionospheric ELF generation

K. Papadopoulos, C. L. Chang, P. Vitello, and A. Drobot

Science Applications International Corporation, McLean, Virginia

(Received June 1, 1988; revised February 21, 1989; accepted November 9, 1989.)

The scaling laws that control the efficiency of converting ground-based HF power to ELF power by using modulation of the polar electrojet current is discussed. The analysis is based on kinetic calculations of the modification of the ionospheric conductivity by HF waves in conjunction with the experimental results reported from the Tromso Max Planck and the Alaska high power auroral simulation (HIPAS) facilities. It is shown that the efficiency can be increased by more than a factor of  $10^4$  by (1) using phasing to sweep the antenna beam over an area spanned by a maximum tilt of  $35^\circ$ , on a time scale faster than the cooling rate at the heating altitude ( $<100 \mu\text{s}$ ) and (2) localization of the heating at the E region (90–100 km) where electron runaway can be induced resulting in substantial modification of the Pederson conductivity.

### 1. INTRODUCTION

Generating ULF/VLF/ELF waves by utilizing the ionosphere as an active medium is an exciting prospect. The technique provides frequency agility and avoids many of the geopolitical and economic difficulties associated with large and inefficient ground-based facilities. By adjusting the HF beam geometry, the low-frequency waves can be made to propagate upward in the magnetosphere for use in active magnetospheric stimulation experiments or downward into the Earth's ionosphere waveguide for communication and geological-probing purposes. One of the mechanisms discussed for down-converting HF power to ULF/ELF/VLF power by interaction with the ionosphere requires the presence of ambient ionospheric currents, such as the auroral or equatorial electrojets [Germantsev *et al.*, 1974; Kotik and Trakhtengerts, 1975; Stubbe and Kopka, 1977; Chang *et al.*, 1981; Ferraro *et al.*, 1982], while another relies on pure plasma nonlinearities and does not require the presence of ionospheric currents [Papadopoulos *et al.*, 1982, 1983; Papadopoulos and Chang, 1985; Ko *et al.*, 1986; Ganguli *et al.*, 1986]. Although both mechanisms have been verified experimentally, the predominance of the experiments dealt with the modulation of ionospheric currents because this technique demands lower HF transmitter power and antenna directionality.

Generation of ULF/ELF/VLF waves by modulating ionospheric currents has been confirmed for both the equatorial and the auroral electrojet in experiments conducted in the USSR [Migulin and Gurevich, 1985; Belyaev *et al.*, 1987], the Max-Planck Tromso facility [Stubbe *et al.*, 1982a, b; Barr and Stubbe, 1984a, b; James *et al.*, 1984; Barr *et al.*, 1985], and the United States [Ferraro *et al.*, 1982; Ferraro and Lee, this issue]. Most of the experiments were performed using HF frequencies in the range of 2–5 MHz, while the power density at the interaction region varied between  $10^{-4}$  and  $10^{-3} \text{ W/m}^2$ . The most exhaustive studies were performed at the Tromso Max-Planck facility and the typical results are summarized in Figure 1. These results are in general terms consistent with results produced at other facilities, [Ferraro and Lee, this issue; Belyaev *et al.*, 1987] although the precise values of the detected field amplitudes depend on local conditions, characteristics of the HF facility, and other specific factors. The purpose of this paper is to explore the potential and the limitations of the ionospheric generation of ULF/ELF/VLF waves using as a guide the current experimental results in conjunction with theoretical extrapolations. Namely, starting from the current experimental and theoretical status, we develop scaling laws and use them to explore the efficiency with which HF power can be converted to the desired low-frequency range. It is expected that the conclusions will be useful in guiding future facilities and experiments. For specificity we selected for our study the ELF frequency range (i.e., 50–500 Hz),

Copyright 1990 by the American Geophysical Union.

Paper number 89RS03537.  
0048-6604/90/89RS-03537\$08.00

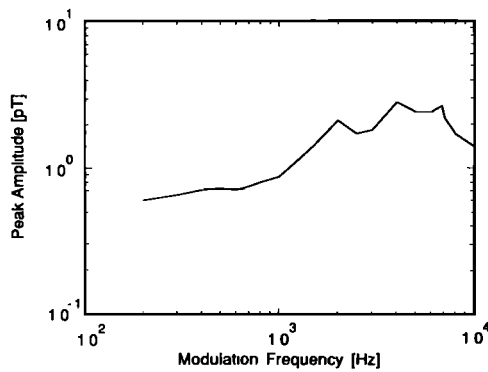


Fig. 1. Typical experimental results in the ELF region generated by the Max Planck Tromso facility [Stubbe *et al.*, 1982].

since in this range the interpretation of the results is not complicated by waveguide resonances, high-order modes, and skin layer thickness. The plan of the paper is as follows. The next section summarizes the status of understanding of ELF generation by current modulation and the resulting scaling laws. Section 3 discusses the level of conductivity modification as a function of the incident power density and altitude. Contrary to previous studies which used fluid analysis to calculate the electron heating, a completely kinetic treatment is used here. Such a treatment is required for power densities exceeding  $10^{-3}$  W/m<sup>2</sup>. Based on the analysis of sections 2 and 3, section 4 discusses techniques for increasing the HF to ELF conversion efficiency. The final section summarizes the results and pinpoints high-leverage research issues.

## 2. IONOSPHERIC ELF GENERATION-SCALING CONSIDERATIONS

Relating the amplitude of the ELF waves on the ground to the extent and characteristics of the modified region in the ionosphere and to the design characteristics of the HF transmitter is a complex problem. Aspects of the problem have been examined by many authors [Kotik and Trakhtengerts, 1975; Bellyustin and Polyakov, 1977; Tripathi *et al.*, 1982; Fejer and Krenzien, 1982; Barr and Stubbe, 1984a, b]. It involves the following series of sequential steps. Based on the transmitter characteristics (power, gain, HF frequency, and modulation frequency) and the applicable model of the ambient ionosphere the conductivity modulation is first computed as a function of altitude. This allows for

the calculation of the modulated current altitude profile, for any specified ambient ionospheric electric field (assumed or measured). This calculation involves computation of the primary current, the polarization currents required to set up quasineutrality, and the induction currents caused by the time dependence of the magnetic field. Finally, from the modulated current profile the excitation and propagation of the ULF/ELF/VLF waves in the Earth's ionospheric waveguide can be computed by using either the extended source technique [Tripathi *et al.*, 1982] or with an equivalent ULF/ELF/VLF moment in the ionosphere the reciprocity principle [Galejs, 1968, 1971; Barr and Stubbe, 1984a, b]. A comprehensive analysis of these factors lies beyond the scope of this paper. Within the experimental and theoretical uncertainties our purpose can be accomplished by starting from the current experimental results in the frequency range of 50–500 Hz and analyzing them under the assumption that the power generated is proportional to the square of the dipole moment

$$M \equiv IL \quad (1)$$

where  $I$  is the total modulated current contributing to the ELF field on the ground and  $L$  is the linear size of the modulated region. All other factors entering the efficiency calculation will be taken from the available experimental data base. For concreteness the measurements and analysis of the Tromso results [Barr and Stubbe, 1984a] are used as our baseline input. These results are in general agreement to the ones reported from high power auroral simulation (HIPAS) [Ferraro and Lee, this issue]. The range of 50–500 Hz has been selected in order to avoid effects associated with waveguide resonances which arise for frequencies above 1 kHz.

The experimental results indicate that when the heating transmitter operated at a power level of 150 MW ERP the amplitude of the ELF field measured on the ground is  $\sim 100$   $\mu$ V/m or 1 pT. These correspond to about 10–100 mW of radiated ELF power in the 200–500 Hz range [Barr and Stubbe, 1984a]. The equivalent radiating horizontal dipole at 75–80 km altitude in the ionosphere is  $IL \approx 3\text{--}5 \times 10^4$  A-m which corresponds to an equivalent ground-based electric vertical dipole with  $IL \approx 2\text{--}4 \times 10^3$  A-m. The polarization is consistent with predominance of Hall current modulation. Compu-

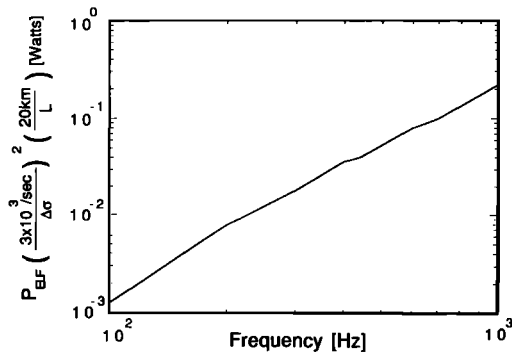


Fig. 2. ELF power versus frequency for the Tromso facility as determined by the analyses of *Barr and Stubbe* [1984a]. The ELF power scale has been multiplied by  $(3 \times 10^3 \text{ s}^{-1}/\Delta\sigma) \times (20 \text{ km}/L)^4$  to emphasize the scaling with size  $L$  and conductivity  $\Delta\sigma$ . For the Tromso results this factor is unity (i.e.,  $\Delta\sigma \approx 3 \times 10^3/\text{s}$ ,  $L \approx 20 \text{ km}$ ).

tations based on a fluid model indicate that for an assumed ambient ionospheric electric field  $E_a = 25 \text{ mV/m}$  the peak values of the modulated current density are in the range of  $10^{-8} \text{ A/m}^2$  and are located between 75 and 80 km in altitude. The effective horizontal radiated current moment  $M$  can be estimated by height integration as

$$M = IL = \Delta j \Delta z L^2 = \Delta\sigma \Delta z E_a L^2 \quad (2)$$

where  $\Delta j$  is the modulated current density,  $\Delta z$  is the extent of the effective radiating layer in altitude, and  $\Delta\sigma$  is the modulated conductivity. For the typical experimental conditions  $L \approx 20 \text{ km}$  (i.e., at a heater beam width of  $15^\circ$ ),  $\Delta z \approx 10 \text{ km}$ , and  $E_a \approx 25 \text{ mV/m}$ , the value of  $IL \approx 3\text{--}5 \times 10^4 \text{ A}\cdot\text{m}$  corresponds to a peak value of  $\Delta\sigma \approx 3\text{--}4 \times 10^3 \text{ s}^{-1}$ . This is achieved with an incident HF power density of  $2 \text{ mW/m}^2$  at 75–80 km height. Finally, it should be noted that the value of  $IL$  is independent of frequency and the frequency dependence in the ELF power is attributed to the scaling of the excitation efficiency [Galejs, 1971].

Since the quantities that can be controlled from the ground are the value (and possibly the altitude location) of the conductivity modulation  $\Delta\sigma$  and the size  $L$ , it is instructive to cast the experimental data as interpreted by *Barr and Stubbe* [1984a] in the form of Figure 2. Notice the important scaling valid for each ELF frequency, i.e.,

$$P_{\text{ELF}} \sim M^2 \sim (\Delta\sigma)^2 L^4 \quad (3)$$

For instance, if we increase the peak conductivity modulation by a factor of 10 while keeping  $L \approx 20 \text{ km}$ , the radiated power at 500 Hz would increase from 100 mW to about 10 W. Similarly, if we increase the size  $L$  by a factor of 5 while keeping  $\Delta\sigma \approx 3\text{--}4 \times 10^3 \text{ s}^{-1}$ , the radiated power would increase by a factor of  $(5)^4 \sim 6 \times 10^2$ .

A critical input needed for the determination of the factors that optimize  $P_{\text{ELF}}$  is the scaling of the conductivity modification  $\Delta\sigma$  on the HF power density  $S$  at the modified height,

$$S \equiv P_{\text{HF}}/L^2 \quad (4)$$

where  $P_{\text{HF}}$  is the ground HF power and  $L$  is the spot size at the appropriate height. Of course this neglects absorption at lower heights, a point that we will return later on. Assuming that

$$\Delta\sigma \sim [P_{\text{HF}}/L^2]^\alpha \quad (5)$$

we find from (3)–(5) that

$$P_{\text{ELF}} \sim P_{\text{HF}}^{2\alpha} L^{4(1-\alpha)} \quad (6)$$

For  $\alpha \approx 1$  we find that  $P_{\text{ELF}}$  is independent of the antenna gain and scales as

$$P_{\text{ELF}} \sim P_{\text{HF}}^2 \quad (7)$$

Namely, the HF to ELF conversion increases as the square of the HF power. For  $\alpha \gg 1$  the ELF conversion efficiency increases enormously by increasing the ground-based HF power  $P_{\text{HF}}$  while maintaining the same antenna gain (i.e.,  $L = \text{constant}$ ). For  $\alpha \ll 1$ , more efficient conversion requires large spot sizes. A computation of the value of  $\alpha$  for various altitudes and HF power densities is performed in the next section.

### 3. DEPENDENCE OF CONDUCTIVITY MODIFICATION ON ALTITUDE AND POWER DENSITY

In this section we evaluate the level of conductivity modulation at various ionospheric heights as a function of the incident HF power density  $S$ . The calculation is “local” and neglects transport. From the modulated conductivity we can easily evaluate the modulated current for a given ionospheric electric field. Contrary to previous studies [Stubbe and Kopka, 1977; Tomko, 1981; Chang et al., 1981; James, 1985] which used fluid equations to compute the variation of the electron temperature  $T_e$  as a

linear approximation, the present study uses the complete time dependent kinetic equation for the electron energy distribution function  $f(\epsilon)$ . For an HF electric field of peak amplitude  $E_o$  and frequency  $\omega_o$  at the chosen height,  $f(\epsilon)$  is given by [Gurevich, 1978]

$$(\partial/\partial t)f(\epsilon) = \epsilon^{-1/2}\partial/\partial\epsilon[\epsilon^{3/2}D(2f/2\epsilon)] - \mathcal{L}(\epsilon) \quad (8)$$

$$D(\epsilon) = \frac{1}{6}(e^2E_o^2/m)\nu(\epsilon)[(\omega_o \pm \Omega)^2 + \nu^2(\epsilon)]^{-1} \quad (9)$$

where  $\nu(\epsilon)$  is the energy dependent electron-neutral collision frequency at the chosen height and  $\Omega$  is the electron cyclotron frequency. The  $\pm$  signs correspond to  $o(+)$  and  $x(-)$  mode heating correspondingly. The term  $\mathcal{L}(\epsilon)$  is an operator that represents the energy loss due to various inelastic processes. Its form is discussed in the appendix and includes excitation of rotational, vibrational, and optical levels as well as ionization and attachment for  $N_2$  and  $O_2$ . Note that the latter process is not important for the power densities analyzed here. Equation (8) was solved numerically for  $f(\epsilon, t)$  at various altitudes, HF power density values  $S$  and modulation frequencies  $\omega$ . The form of  $\nu(\epsilon)$  and the numerical method for solving (8) are given in the appendix. The time dependence of the conductivity is found from

$$\sigma_p(t) = \frac{ne^2}{m} \int \frac{\nu(\epsilon)}{\Omega^2 + \nu^2(\epsilon)} f(\epsilon, t) \epsilon^{1/2} d\epsilon \quad (10a)$$

$$\sigma_h(t) = \frac{ne^2}{m} \int \frac{\Omega}{\Omega^2 + \nu^2(\epsilon)} f(\epsilon, t) \epsilon^{1/2} d\epsilon \quad (10b)$$

$$\sigma_z(t) = \frac{ne^2}{m} \int \frac{1}{\nu(\epsilon)} f(\epsilon, t) \epsilon^{1/2} d\epsilon \quad (10c)$$

where  $\sigma_p$ ,  $\sigma_h$ , and  $\sigma_z$  are the Pederson, Hall, and parallel conductivities and  $n$  is the electron density. As noted in the introduction a kinetic analysis is an absolute requirement for exploring high-power densities. The initial  $f(\epsilon, t = 0)$  was taken as Maxwellian at  $T_e \approx 0.025$  eV. For the studies reported below  $\omega_o = 1.8 \times 10^7$  rad/s which corresponds to a heater frequency of 2.8 MHz.

We report below results for daytime ionospheric conditions corresponding to altitudes between 70 and 100 km. The ionospheric model used is shown in Figure 3.

The need for a kinetic description at high power

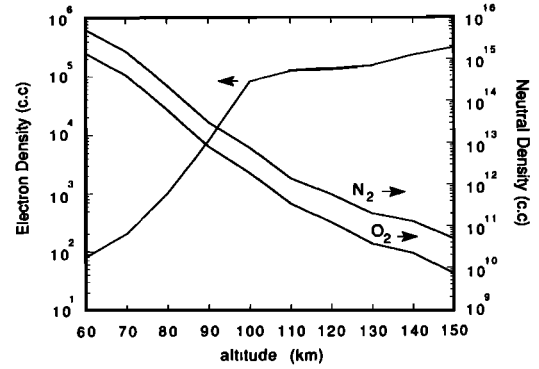


Fig. 3. Ionospheric profile used in the Fokker-Planck runs.

and high altitude is obvious from the distribution function shown in Figure 4. Figures 4a–4c show the initial and steady state distribution functions for ionospheric heating at 75, 90, and 100 km altitude and at values of  $S = 10^{-3}$  W/m<sup>2</sup>,  $10^{-2}$  W/m<sup>2</sup>, and  $10^{-2}$  W/m<sup>2</sup>, correspondingly. The time required to reach steady state was in all cases much shorter than  $10^{-4}$  s. This implies that steady state is reached at times much shorter than the relevant modulation frequencies. It is seen that at low-altitude and low-power density (i.e., 75 km,  $10^{-3}$  W/m<sup>2</sup>)  $f(\epsilon)$  does not deviate much from Maxwellian and the fluid description is a reasonable approximation. This, however, is not true for the other two cases where the high-energy tails of the distribution functions become the dominant part.

Figures 5–6 show the time dependence of the Hall and Pedersen modulation for the above three cases. At 75 km and  $10^{-3}$  W/m<sup>2</sup> the Hall conductivity modulation is about  $7 \times 10^3$  s<sup>-1</sup> which is consistent with the value quoted in section 2 for the Tromsø experiments. The Pederson conductivity modulation is significantly smaller. This is reversed for the 90 and 100 km cases at  $10^{-2}$  W/m<sup>2</sup>. The Hall conductivity modulation becomes progressively smaller and is negligible at 100 km. Furthermore, the level of the Pederson conductivity modulation is about  $3 \times 10^4$  s<sup>-1</sup> at 90 km and  $6 \times 10^4$  s<sup>-1</sup> at 100 km. It is clear that if the size  $L$ , which is controlled by the antenna gain was the same for all three cases and the increase in the power density was entirely due to an increase in  $P_{HF}$  by a factor of 10, the radiated  $P_{ELF}$  would increase by a factor of 20 and 100 for the 90 and 100 km cases over the 75 km case. Notice that since steady state is established for all cases much earlier than the low-frequency oscilla-

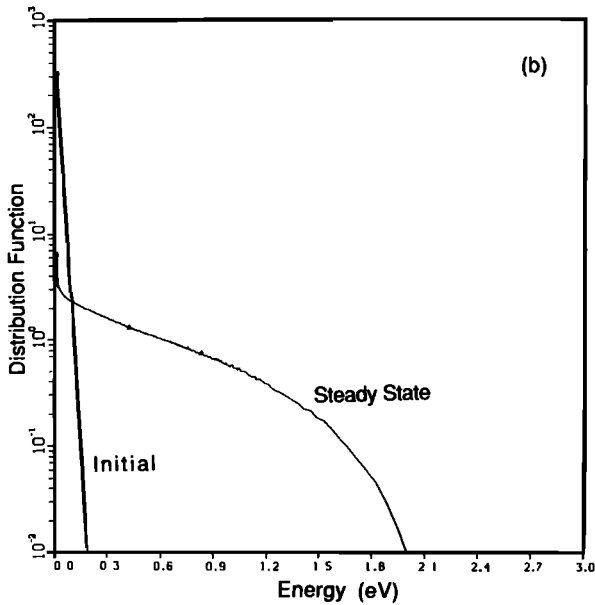
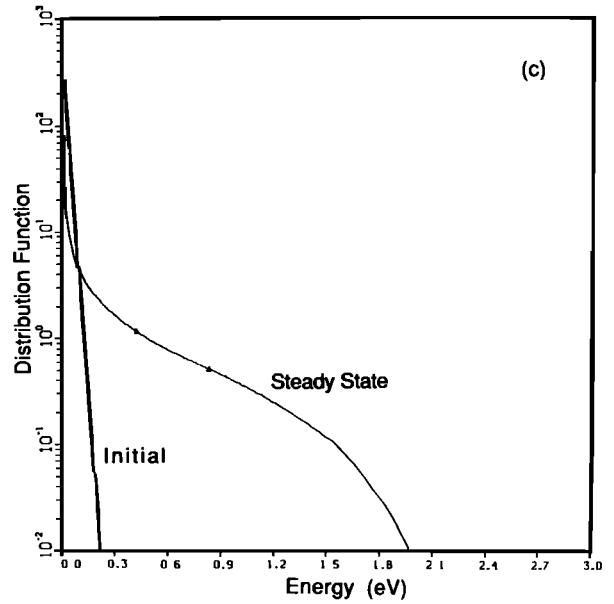
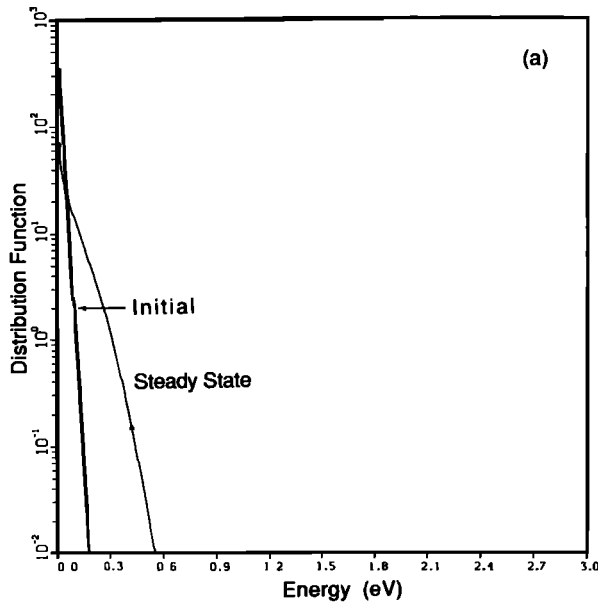


Fig. 4. (continued)

Fig. 4. Initial and steady state electron distribution for (a) 75 km,  $S = 10^{-3} \text{ W/m}^2$ ; (b) 90 km,  $S = 10^{-2} \text{ W/m}^2$ ; and (c) 100 km,  $S = 10^{-2} \text{ W/m}^2$ .

$10^{-4} \text{ W/m}^2$ . The results for the Hall and Pederson conductivities are shown in Figures 7 and 8. The boundary altitudes were chosen in a way that they reflect the range of variation of the Pedersen and Hall conductivities with altitude. A more detailed analysis of the consequences of the results shown in Figures 7 and 8 and of the efficiency optimization at intermediate altitudes will be presented elsewhere. We restrict our discussion here to the consequences of the general trends derived from Figures 7 and 8. These are:

1. For low altitudes ( $\sim 70\text{--}75$  km) the Hall conductivity provides the dominant contribution. The value of  $\Delta\sigma_h$  increases very weakly with power density ( $\alpha < 1/2$ ) and saturates at a value of  $S$  about  $10^{-3} \text{ W/m}^2$ . Further increase in the power density does not produce any increase in the modulated current density. According to the discussion after (7), optimization of the conversion efficiency requires increase in  $L$  under constant  $S$ .

2. For high altitude ( $>90$  km) heating the modification of the Pederson conductivity dominates. The value of  $\Delta\sigma_p$  increases as  $S^2$  (i.e.,  $\alpha = 2$ ), up to power density of  $10^{-2} \text{ W/m}^2$  and saturates slowly afterward. There is an obvious premium in increasing  $P_{\text{HF}}$ , since in this case  $P_{\text{ELF}} \sim P_{\text{HF}}^4$ , while keeping  $S = 10^{-2} \text{ W/m}^2$ .

tion period, the values of  $\Delta\sigma$  are independent of the ELF frequency. In order to determine the scaling of the conductivity modification with power density and altitude we conducted a survey of the level of steady conductivity modification for altitudes (70 and 100 km) and values of  $S$  in the range of

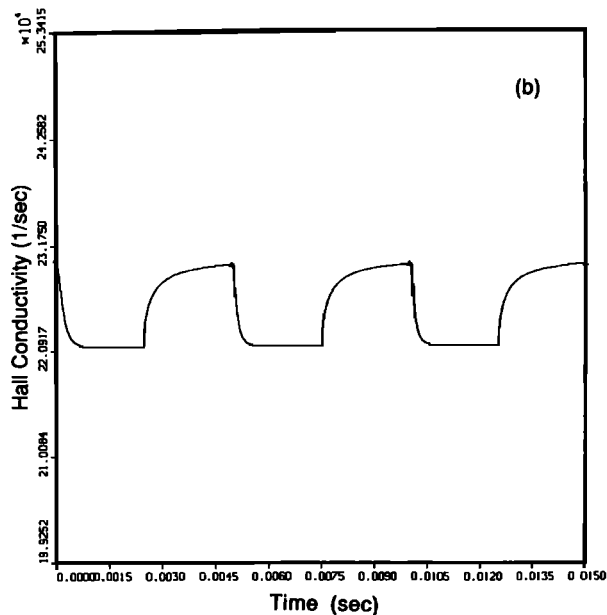
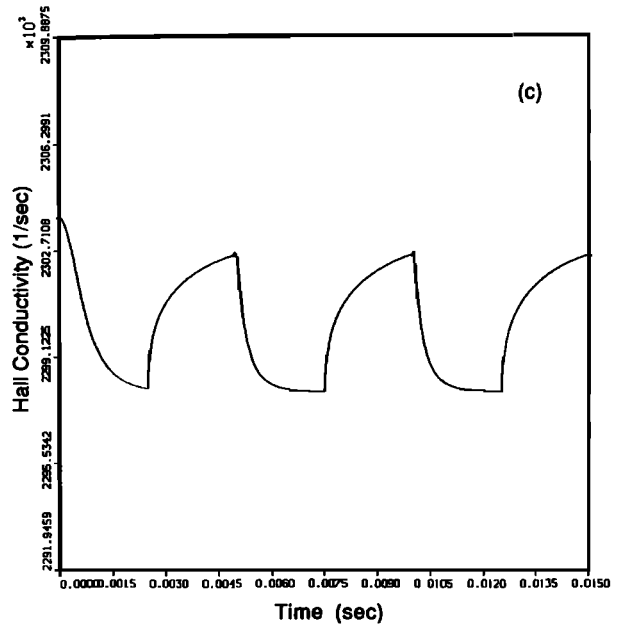
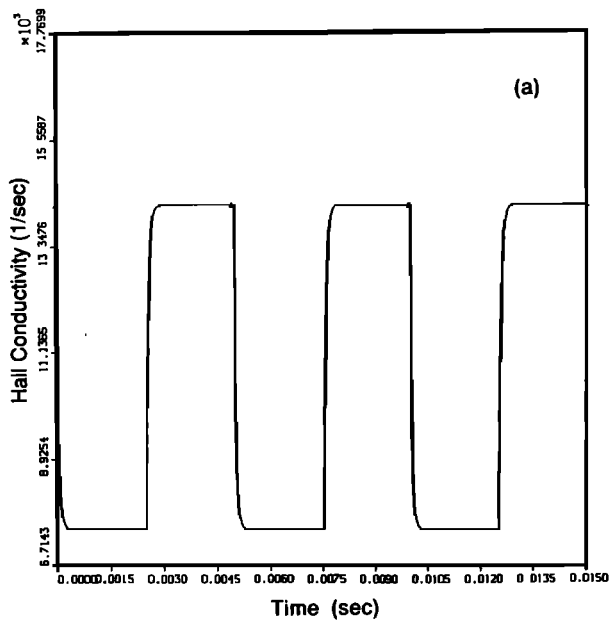


Fig. 5. Hall conductivity modification for the cases of Figure 4.

3. Maximum value of  $\Delta\sigma$  is achieved for high-altitude heating.

Note that in Figure 7, the  $|\Delta\sigma_h|$  curve at 100 km shows a dip near the power level of  $0.4 \text{ W/m}^2$ . This implies a sign change of  $\Delta\sigma_h$  from minus to plus as the heating power increases at high altitude. This

Fig. 5. (continued)

interesting feature is a direct result of using the kinetic approach to estimate Hall conductivity. Specifically, at high-altitude and high heating power, the energy integral in (10b) gives an overall positive contribution to  $\sigma_h$  as the electron distribution shifts toward the high energy end. In contrast, the conventional fluid approach always predicts a decrease in  $\sigma_h$  since the collision frequency  $\nu(Te)$  increases with the fluid temperature  $Te$ .

Before closing this section we should caution the reader in the interpretation of the above results. In order to have uniformity in the results and be close to the benchmark case, the survey shown in Figure 4 was performed using the same frequency  $\omega_o = 1.8 \times 10^7$  for all the three altitudes examined (75, 90, 100 km). This frequency corresponds to a critical electron density  $n_c = 10^5$  electrons/cm<sup>3</sup> which corresponds to an altitude of 105 km for the model ionosphere used here. The electron densities at 75, 90, and 100 km (Figure 3) are  $3 \times 10^2$  electrons/cm<sup>3</sup>,  $8 \times 10^3$  electrons/cm<sup>3</sup>, and  $8 \times 10^4$  electrons/cm<sup>3</sup>. Since the code does not include collective effects, the 100 km results are close but within the validity range of the model. Furthermore, as long as the half width of the heater is smaller than  $26^\circ$ , effects of resonance absorption can also be neglected even for the 100 km case. However, we

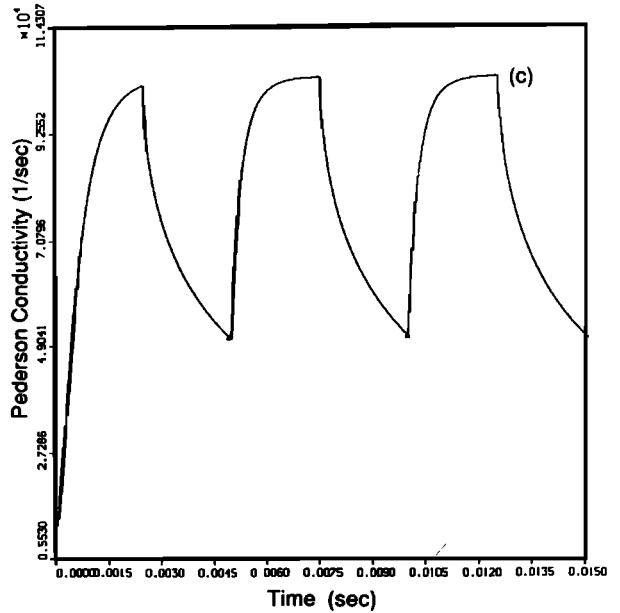
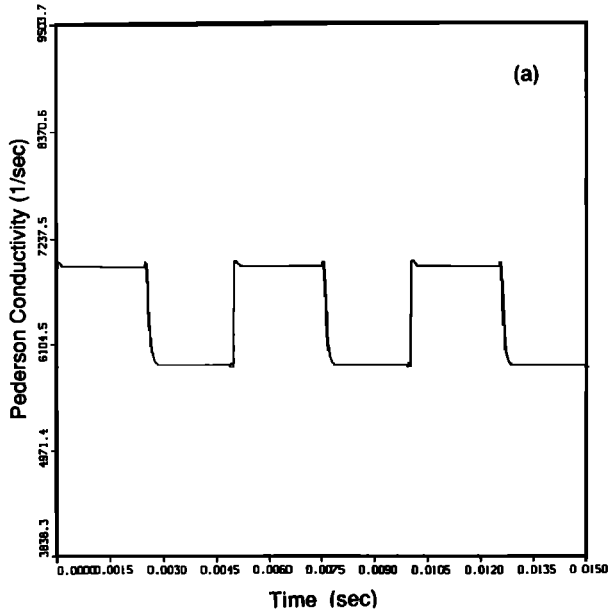


Fig. 6. (continued)

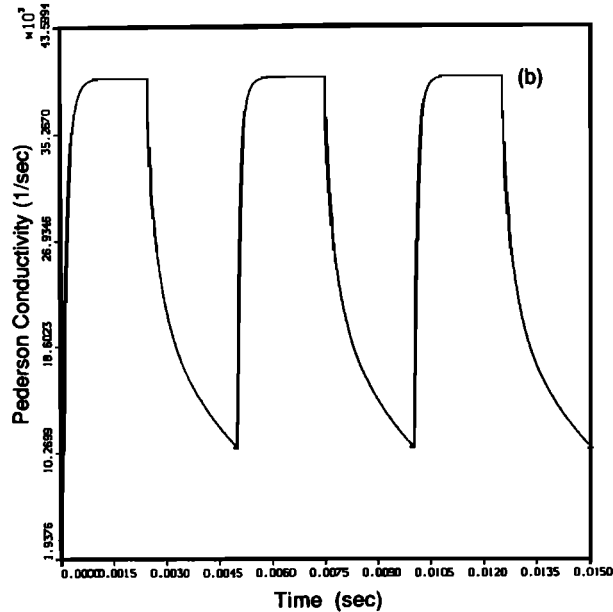


Fig. 6. Same as Figure 5 for the Pederson conductivity.

should note that for the high altitude cases ( $>90$  km) the results are applicable to frequencies higher than the 2.8 MHz by a simple scaling law based on (8) and (9). Note that for  $\omega_o > 2.8$  MHz and  $h > 90$  km,  $(\omega_o \pm \Omega)^2 \gg \nu(\epsilon)$ . Therefore

$$D(\epsilon) = \frac{1}{3} \bar{\epsilon} \nu(\epsilon) \tag{11}$$

where  $\bar{\epsilon}$  is the quiver energy of the electrons in the high-frequency field, with an effective frequency  $\omega_{\text{eff}} = \omega_o \pm \Omega$ , defined as

$$\bar{\epsilon} = \frac{1}{2} m(eE_0/m\omega_{\text{eff}})^2 \tag{12}$$

Our results can be generalized to any frequency by noting that the solution of (8) is self-similar with respect to the value of  $\bar{\epsilon}$ . Thus for a frequency  $\omega > \omega_o$  a power density is higher by a factor  $(\omega \pm \Omega)^2/(\omega_o \pm \Omega)^2$  than for  $\omega = \omega_o$  will be required.

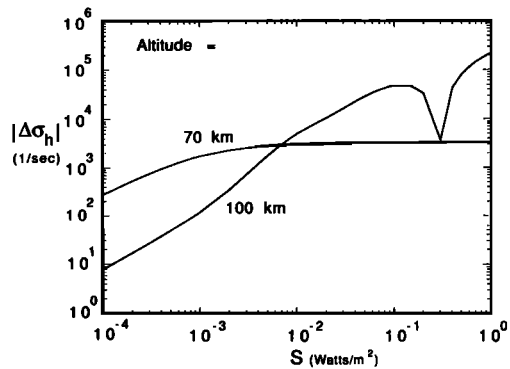


Fig. 7. Hall conductivity modulation versus  $S$  for 70 and 100 km.

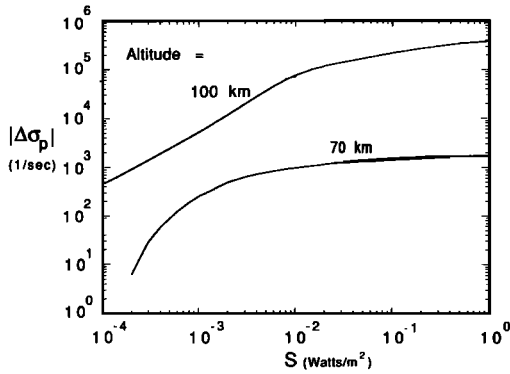


Fig. 8. Pederson conductivity modulation versus  $S$  for 70 and 100 km.

#### 4. EFFICIENCY OF HF TO ELF CONVERSION

In this section we combine the results of *Barr and Stubbe* [1984a] as shown in Figure 2 with the results reported in section 3 and use them to determine the HF to ELF conversion efficiency and techniques by which it can be optimized. On the basis of Hall conductivity modulation of the polar electrojet at 70–75 km altitude, *Barr and Stubbe* [1984a] estimate a power conversion efficiency of 5–10 mW per MW of HF at 200 Hz. This implies an overall conversion efficiency of about  $10^{-8}$ , compared with  $10^{-6}$  conversion achieved by the Wisconsin Test Facility. For low-altitude heating the results of section 3 indicate that increasing the power does not have any significant effect in the ELF power. However, as shown in (3) for constant power density and therefore constant  $\Delta\sigma$ ,  $P_{\text{ELF}} \sim L^4$ . An increase in area while maintaining approximately the same power density can be achieved by using phasing to sweep the antenna beam over an area spanned by a maximum tilt of  $\theta_m^\circ$  in each direction at a rate faster than the cooling rate, which for 80 km is approximately few microseconds.  $P_{\text{ELF}}$  will increase according to (3) by a factor of  $(\tan(\theta_m + \theta_o)/\tan \theta_o)^4$ . Taking  $\theta_o = 7.5^\circ$  and  $\theta_m = 35^\circ$ , we find an increase on the ELF power by a factor of  $2 \times 10^3$ . Thus a facility of the type of Tromso or HIPAS equipped with fast sweeping over a cone of  $35^\circ$  can produce 5–10 watts of ELF power and can have an efficiency of  $10^{-5}$  which is better than the efficiency of the Navy ELF Wisconsin test facility.

Alternately, higher efficiency as well as higher  $P_{\text{ELF}}$  can be produced by high-altitude heating. If HF heating localized in the 95–100 km region can be

achieved with power density of the order of 10 mW/m<sup>2</sup>, the resultant conductivity modification according to Figures 7 and 8 increases by a factor of 100 over that for low-altitude heating. According to (3), this will produce a factor of  $10^4$  more power than the 5–10 mW, which results in 50–100 W in ELF even in the absence of sweeping. The system efficiency increases by a factor of  $10^3$  giving an overall conversion efficiency of  $10^{-5}$ . Incorporating a similar sweep as for the low-altitude heating will result in further increase of the efficiency by a factor of 400 giving an overall efficiency better than  $4 \times 10^{-3}$ . The practical difficulty in realizing the high-altitude scheme, especially under day time conditions, is the fact that self absorption at lower heights could prevent the achievement of power densities of 10 mW/m<sup>2</sup> at 95–100 km altitude for frequencies of 2.8 MHz used in our calculations. Such heating can be achieved by using higher frequencies, beating two HF waves at the local plasma frequency, or using short pulses that allow the power to “sneak through” to high altitudes. These possibilities are currently under study. The enormous increase in efficiency achieved in high-altitude heating places a large premium in realizing them even if their efficiency is by an order of magnitude lower.

#### 5. SUMMARY AND CONCLUSIONS

We presented a detailed kinetic study of local heating of the ionospheric plasma by modulated radiowaves, of the resultant conductivity modulation and of the associated modulated current density in the presence of an ionospheric electric field in the ELF region (50–500 Hz). Regimes where the conductivity modulation is a strong or weak function of the incident HF power density were identified. Combining these results with the recorded observations in this ELF region and assuming that to zero order the ELF power density is proportional to  $(\Delta\sigma)^2 L^4$  we found that the HF to ELF power conversion efficiency can be increased by more than 2 orders of magnitude if the heater could be swept over a  $35^\circ$  cone on timescales faster than the plasma cooling rate ( $\sim 10 \mu\text{s}$ ) for low-altitude heating. Heating techniques that can preferentially deposit their energy at higher altitude ( $\sim 90$ – $100$  km) where the dominant modulated current is the Pederson current, can further increase the efficiency by a factor of  $10^4$ , although part of this increase can be negated by the potential inefficiency of high-altitude

heating as well as by a more inefficient coupling to the waveguide. We are currently examining these issues theoretically and expect to resolve them in combination with the Penn State HIPAS experimental campaigns.

#### APPENDIX

The inelastic term  $\mathcal{L}(\varepsilon)$  in the Fokker-Planck equation (equation (8)) is a summation of the various inelastic collision contributions

$$\mathcal{L}(\varepsilon) = S_r + S_{v,o} + S_a + S_i \quad (\text{A1})$$

Detailed expressions of these inelastic contributions are given as follows [Gurevich, 1978]:

Excitation of rotational levels

$$S_r = \frac{1}{2v^2} \frac{\partial}{\partial v} \left[ v^2 R_r(v) \left( \frac{T}{m} \frac{\partial f}{\partial v} + vf \right) \right] \quad (\text{A2})$$

where

$$R_r(v) = 8B_o \sigma_o N_m / mv$$

$$\sigma_o = 8\pi Q^2 a_o^2 / 15$$

$$a_o = h^2 / me^2 \quad \text{Bohr radius}$$

$$Q = 1.04 \quad \text{for } N_2$$

$$Q = 1.80 \quad \text{for } O_2$$

$$B_o = 2.48 \times 10^{-4} \text{ eV} \quad \text{for } N_2$$

$$B_o = 1.79 \times 10^{-4} \text{ eV} \quad \text{for } O_2$$

$N_m$  is the number density of  $N_2$  and  $O_2$ , and  $S_r$  is summing over both  $N_2$  and  $O_2$  species.

Excitation of vibrational and optical levels

$$S_{v,o} = -\frac{2N_m}{mv} \sum_k [(\varepsilon + \varepsilon_k) f(\varepsilon + \varepsilon_k) \sigma_k(\varepsilon + \varepsilon_k) - \varepsilon f(\varepsilon) \sigma_k(\varepsilon)] \quad (\text{A3})$$

where  $k$  stands for different levels,  $\sigma_k$  is the energy of the  $k$  state, and  $\sigma_k$  is the cross section.

Attachment

$$S_a = -N_o v \sigma_a f \quad (\text{A4})$$

where  $\sigma_a$  is the attachment cross section and  $N_o$  is the  $O_2$  number density.

Ionization

$$S_i = -\frac{2N_m}{mv} \left[ \int_{\varepsilon_i}^{\infty} f(\varepsilon, \varepsilon_p) \varepsilon_p f(\varepsilon_p) \sigma_i(\varepsilon_p) d\varepsilon_p - \varepsilon f(\varepsilon) \sigma_i(\varepsilon) \right] \quad (\text{A5})$$

where  $\varepsilon_i$  is the ionization energy and  $\sigma_i$  is the ionization cross section.

The collision frequency  $\nu(\varepsilon)$  used in (9) contains the elastic collisions of the electrons with the neutral molecules. As such, the  $\nu(\varepsilon)$  can be written as

$$\nu(\varepsilon) = \sum_m N_m \nu \sigma_m(\varepsilon) \quad (\text{A6})$$

where  $N_m$  is the neutral density at the chosen height,  $\sigma_m$  is the momentum transfer cross section, and the summation is carried over both  $O_2$  and  $N_2$  species.

Numerically, a finite difference scheme for initial value problems of Fokker-Planck equations has been applied to solve the governing equation (equation (8)). Details of the numerical method can be found in the work by Chang *et al.* [1970].

*Acknowledgments.* The work was supported by the Office of Naval Research through Penn State subcontract ONR-TPSU-SAIC 0677-388. Discussions with Ferraro and Lee of Penn State and Ossakow of the Naval Research Laboratory are gratefully acknowledged.

#### REFERENCES

- Barr, R., and P. Stubbe, The "polar electrojet antenna" as a source of ELF radiation in the Earth-ionosphere waveguide, *J. Atmos. Terr. Phys.*, **46**, 315-320, 1984a.
- Barr, R., and P. Stubbe, ELF and VLF radiation from the "polar electrojet antenna," *Radio Sci.*, **19**, 1111-1122, 1984b.
- Barr, R., M. T. Rietveld, P. Stubbe, and H. Kopka, The diffraction of VLF radio waves by a patch of ionosphere illuminated by a powerful HF transmitter, *J. Geophys. Res.*, **90**, 2861-2875, 1985.
- Bellyustin, N. S., and S. V. Polyakov, Propagation of low-frequency electromagnetic waves in the Earth-ionosphere waveguide, *Radiophys. Quantum Electron.* Engl. Transl., **20**, 57-64, 1977.
- Belyaev, P. P., D. S. Kotik, S. N. Mityakov, S. V. Polyakov, V. O. Rapoport, and V. Yu. Trakhtengerts, Generation of electromagnetic signals at combination frequencies in the ionosphere, *Radiophys. Quantum Electron.* Engl. Transl., **30**, 189-206, 1987.

- Chang, C. L., V. Tripathi, K. Papadopoulos, J. Fedder, P. J. Palmadesso, and S. L. Ossakow, *Effect of the Ionosphere on Radiowave Systems*, edited by J. M. Goodman, p. 91, U.S. Government Printing Office, Washington, D. C., 1981.
- Chang, J. S., and G. Cooper, A practical difference scheme for Fokker-Planck equations, *J. Comp. Phys.*, **6**, 1-16, 1970.
- Fejer, J. A., and E. Krenzien, Theory of generation of ULF pulsations by ionospheric modification experiments, *J. Atmos. Terr. Phys.*, **44**, 1075-1087, 1982.
- Ferraro, A. J., H. S. Lee, Determination of the D region electron density from the ELF frequency stepping experiment, *Radio Sci.*, this issue.
- Ferraro, A. J., H. S. Lee, R. Allshouse, K. Carroll, A. A. Tomko, F. J. Kelly, and R. G. Joiner, VLF/ELF radiation from the ionospheric dynamo current system modulated by powerful HF signals, *J. Atmos. Terr. Phys.*, **44**, 1113-1122, 1982.
- Galejs, J., Propagation of ELF and VLF waves below an anisotropic ionosphere with a dipping static magnetic field, *J. Geophys. Res.*, **73**, 339-352, 1968.
- Galejs, J., Excitation of the terrestrial waveguide by sources in the lower ionosphere, *Radio Sci.*, **6**, 41-53, 1971.
- Getmantsev, G. G., N. A. Zuikov, D. S. Kotik, L. F. Mironenko, N. A. Mityakov, V. O. Rapoport, Yu. A. Sazonov, V. Yu. Trakhtengerts, and V. Ya. Eidman, Combination frequencies in the interaction between high power short-wave radiation and ionospheric plasma, *JETP Lett. Engl. Transl.*, **20**, 101-102, 1974.
- Gurevich, A. V., *Nonlinear Phenomena in the Ionosphere*, Springer-Verlag, New York, 1978.
- James, H. G., The ELF spectrum of artificially modulated D/E-region conductivity, *J. Atmos. Terr. Phys.*, **47**, 1129-1142, 1985.
- James, H. G., R. L. Dowden, M.T. Rietveld, P. Stubbe, and H. Kopka, Simultaneous observations of ELF waves from an artificially modulated auroral electrojet in space and on the ground, *J. Geophys. Res.*, **89**, 1655-1666, 1984.
- Ko, K., C. R. Menyuk, A. Reiman, V. Tripathi, P. Palmadesso, and K. Papadopoulos, ELF generation in the lower ionosphere via collisional parametric decay, *J. Geophys. Res.*, **91**, 10,097-10,107, 1986.
- Kotik, D. S., and V. Yu. Trakhtengerts, Mechanism of excitation of combination frequencies in ionospheric plasma, *JETP Lett. Engl. Transl.*, **21**, 51-52, 1975.
- Migulin, V. V., and A. V. Gurevich, Investigation in the U.S.S.R. of non-linear phenomena in the ionosphere, *J. Atmos. Terr. Phys.*, **47**, 1181-1188, 1985.
- Papadopoulos, K., and C. L. Chang, Generation of ELF/ULF waves in the ionosphere by dynamo processes, *Geophys. Res. Lett.*, **12**, 279-282, 1985.
- Papadopoulos, K., R. Sharma, and V. Tripathi, ELF generation by parametric excitation of Alfvén waves in the ionosphere, *J. Geophys. Res.*, **87**, 1491-1494, 1982.
- Papadopoulos, K., K. Ko, and V. Tripathi, Efficient parametric decay in dissipative media, *Phys. Rev. Lett.*, **51**, 463-466, 1983.
- Stubbe, P., and H. Kopka, Modulation of the polar electrojet by powerful HF waves, *J. Geophys. Res.*, **82**, 2319-2325, 1977.
- Stubbe, P., H. Kopka, and R. L. Dowden, "Generation ELF and VLF waves by polar electrojet modulation: Experimental results, *J. Geophys. Res.*, **86**, 9073-9078, 1981.
- Stubbe, P., H. Kopka, H. Lauche, M. T. Rietveld, A. Brekke, O. Holt, and R. L. Dowden, Ionospheric modification experiments in northern Scandinavia, *J. Atmos. Terr. Phys.*, **44**, 1025-1042, 1982a.
- Stubbe, P., H. Kopka, M. T. Rietveld, and R. L. Dowden, ELF and VLF wave generation by modulated HF heating of the current carrying lower ionosphere, *J. Atmos. Terr. Phys.*, **44**, 1123-1136, 1982b.
- Tomko, A. A., Nonlinear phenomena arising from radio heating of the lower ionosphere, *Rep. PSU-IRL-SCI-470*, Ionos. Res. Lab., Penn. State Univ., University Park, 1981.
- Tripathi, V. K., C. L. Chang, and K. Papadopoulos, Excitation of the Earth-ionosphere waveguide by an ELF source in the ionosphere, *Radio Sci.*, **17**, 1321-1326, 1982.

---

C. L. Chang, A. Drobot, K. Papadopoulos, and P. Vitello, Science Applications International Corporation, 1710 Goodridge Drive, McLean, VA 22102.